



Universidade de São Paulo

Biblioteca Digital da Produção Intelectual - BDPI

Departamento de Física e Ciências Materiais - IFSC/FCM

Artigos e Materiais de Revistas Científicas - IFSC/FCI

2011-04

Growth of silver nano-particle embedded in tellurite glass: interaction between localized surface plasmon resonance and 'Er IND.3+' ions

Optical Materials, Amsterdam : Elsevier, v. 33, n. 6, p. 888-892, Apr. 2011
<http://www.producao.usp.br/handle/BDPI/49640>

Downloaded from: Biblioteca Digital da Produção Intelectual - BDPI, Universidade de São Paulo

Growth and magnetic properties of bulk electron doped $\text{La}_{0.7}\text{Ce}_{0.3}\text{MnO}_3$ manganites

S. Sergeenkov^{*1}, C. A. Cardoso¹, M. R. B. Andreetta², A. C. Hernandez², E. R. Leite³, and F. M. Araújo- Moreira¹

¹Departamento de Física, Grupo de Materiais e Dispositivos, CMDMC, UFSCar, 13565-905 São Carlos, SP, Brazil

²Grupo de Crescimento de Cristais e Materiais Ceramicos, CMDMC, IFSC-USP, 13560-970 São Carlos, SP, Brazil

³Departamento de Química, LIEC, CMDMC, UFSCar, 13565-905 São Carlos, SP, Brazil

Received 12 January 2011, revised 28 February 2011, accepted 7 March 2011

Published online 25 March 2011

Keywords cerium compounds, electron-doped manganites, ferromagnetic phases, laser-heated pedestal growth

* Corresponding author: e-mail sergei@df.ufscar.br, Phone: +55-16-260-8205, Fax: +55-16-260-4835

We report on the growth of bulk samples (composite fibers) of the nominal composition $\text{La}_{0.7}\text{Ce}_{0.3}\text{MnO}_3$ (LCMO) manganites (with Curie temperature $T_{C,\text{max}} = 300$ K) by using the laser heated pedestal growth (LHPG) technique. Samples composition was verified through scanning electron microscopy with energy dispersive X-ray (EDX) analysis. The magnetic

behavior of the fibers was probed by magnetization measurements. In addition to a weak ferromagnetic transition at $T_{C0} = 45$ K (due to MnO_2 impurities), two more transitions with $T_{C1} = 126$ K and $T_{C2} = 180$ K were identified and linked to regions with cerium concentration of $x = 0.063$ and 0.13 , respectively.

© 2011 WILEY-VCH Verlag GmbH & Co. KGaA, Weinheim

1 Introduction Magnetic manganites of the form $\text{R}_{1-x}\text{A}_x\text{MnO}_3$ with $\text{R} = (\text{La}, \text{Pr}, \text{Nd})$ and $\text{A} = (\text{Ca}, \text{Sr}, \text{Ba})$ constitute one of the most fascinating classes of materials, exhibiting a wide variety of structures and properties [1, 2], including colossal magnetoresistance (CMR), due to the presence of the mixed valence of manganese as Mn^{3+} and Mn^{4+} . For different compositions, the Mn–O–Mn bond angle also plays a significant role in determining the Curie temperature T_C [2]. As a matter of fact, the Curie temperature was found to decrease with the reduction of the ionic radius of the divalent metal A^{2+} or of the trivalent rare earth R^{3+} since in both cases there is an increasing distortion in the MnO_6 octahedra [3–7]. Some substantial progress has been made in doping manganite systems with tetravalent ions (like, *e.g.*, cerium) but mainly in the form of thin films [8–21]. The possibility to synthesize bulk electron and hole doped manganites will have a significant impact on designing new hybrid devices which take advantage of both spin and charge degrees of freedom.

In this paper, we present our latest results on the growth, characterization and magnetic properties of polycrystalline fibers of nominal composition $\text{La}_{0.7}\text{Ce}_{0.3}\text{MnO}_3$ (LCMO) grown by the laser heated pedestal growth (LHPG) technique. Our results clearly demonstrate a real possibility to grow cerium doped manganites even in a bulk form.

2 Experimental details The LHPG technique was previously used [22] to grow high-quality single crystals of $\text{La}_{0.7}\text{Ca}_{0.3}\text{MnO}_3$ and the same parameters were adopted in the present work to grow our LCMO samples. Namely, source pedestals of LCMO were initially prepared by mixing in the stoichiometric proportion of high purity La_2O_3 , CeO_2 , and MnO_2 powders. No pre-reaction was done because previous tests on $\text{La}_{0.7}\text{Sr}_{0.3}\text{MnO}_3$ and $\text{La}_{0.7}\text{Ca}_{0.3}\text{MnO}_3$ indicated that crystals of similar quality were obtained whether the pedestal was pre-reacted or not. The powder used for pedestal preparation was cold extruded and the resulting pedestals were allowed to dry in air for 24 h. The growth process was performed in a conventional LHPG system with a CO_2 laser [23]. The fiber and pedestal pulling speed, as well as the laser power, were modulated by an automatic diameter control system [23]. The average pulling speed was 18 mm/h.

3 Results and discussion The obtained fibers are polycrystals with black opaque surfaces. The fibers have a diameter around 1 mm and are up to 30 mm long. A longitudinally polished fiber was examined in a scanning electron microscope (SEM) and its composition was verified by the energy dispersive X-ray (EDX) analysis. Images obtained using backscattered electrons revealed that the fiber

© 2011 WILEY-VCH Verlag GmbH & Co. KGaA, Weinheim

consists of three main compositions. From the seed end of the fiber, we observe a gray matrix with a white precipitate first appearing periodically and later in a continuous way, but always in the form of a small reticulate, as shown in Fig. 1. As we move away from this end of the fiber, we start to observe the appearance of a second phase, which appears as black regions in the SEM images. Interestingly enough, this black phase occurs basically in the central core of the fiber, with some elongated areas growing toward the fiber surface. In this region, we also identify the white phase in the form of elongated areas pointing from the center to the surface of the fiber and getting closer to the surface as the growth of the fiber continued. Finally, in the pedestal end of the fiber, the three phases seem to be mixed (see Fig. 1). However, it is important to emphasize that the gray phase is the dominant one along the entire fiber. In order to identify the composition of these three phases, we performed EDX measurements in different regions of the fiber. In Fig. 2 we present a composition map of a $40\ \mu\text{m} \times 40\ \mu\text{m}$ region in the center of the fiber. It can be seen that the white region is rich in cerium, while the black one is rich in manganese. A quantitative analysis indicates that the white region is indeed cerium oxide, while the black one contains some manganese oxide, with only small traces of lanthanum and no cerium at all. More interesting is the result for the dominant gray region. The quantitative analysis reveals a proportion of 49:39:12 for Mn, La, and Ce, respectively (pointing to a stoichiometry of $\text{La}_{0.76}\text{Ce}_{0.24}\text{Mn}_{0.96}\text{O}_x$) in the pedestal extremity of the fiber, and a proportion of 49:42:09 (equivalent to $\text{La}_{0.82}\text{Ce}_{0.18}\text{Mn}_{0.96}\text{O}_x$ composition) in the seed end of the fiber. The obtained stoichiometries for the gray regions clearly indicate that we do have a bulk configuration of the cerium doped LCMO phase. Furthermore, the fact that the $\text{Mn}/(\text{La} + \text{Ce})$ ratio obtained by EDX is less than unity hints at the presence of vacancies in

the Mn sub-lattice, resulting in the formation of the above-mentioned regions in our samples. It is worth mentioning that the presence of Mn vacancies up to 2 at% in fibers grown by LHPG was previously reported [22].

Now let us turn our attention to the magnetic properties of the fiber. A small piece (3 mm long) was cut from the center of the fiber and its magnetic response was measured as a function of temperature. According to Fig. 3, in addition to the broad transition with the highest Curie temperature $T_{\text{C,max}} = 300\ \text{K}$ (corresponding to the nominal composition [19] LCMO), it is possible to identify three major magnetic transitions around 45, 126, and 180 K indicating the presence of different phases within the measured part of the fiber. Most probably, the transition at $T_{\text{C0}} = 45\ \text{K}$ is associated with a weak ferromagnetic transition due to MnO_2 impurities [11]. Next, according to the proposed [19] phase diagram for $\text{La}_{1-x}\text{Ce}_x\text{MnO}_3$ thin films, we identify two cerium induced ferromagnetic phase transitions at 126 and 180 K corresponding to $x = 0.063$ and 0.13 , respectively.

To better understand the origin of the above-mentioned magnetic transitions in the observed behavior of the spontaneous magnetization in our sample, we adopt the spin polaron scenario for doped manganites (exhibiting CMR like behavior) and assume that the temperature and x dependence of the magnetization is governed by the Curie–Weiss contribution [24, 25]

$$M(T, x) = M_{\text{R}}(x) + M_0(x) \tanh \sqrt{\frac{T_{\text{C}}^2(x)}{T^2} - 1}. \quad (1)$$

Here $T_{\text{C}}(x)$ is the doping dependent Curie temperature with x being a cerium concentration, $M_0(x)$ accounts for the deviation of the saturation magnetization of the undoped material in the presence of Ce atoms, and $M_{\text{R}}(x) = M(T_{\text{C}}(x), x)$ is a residual contribution from the

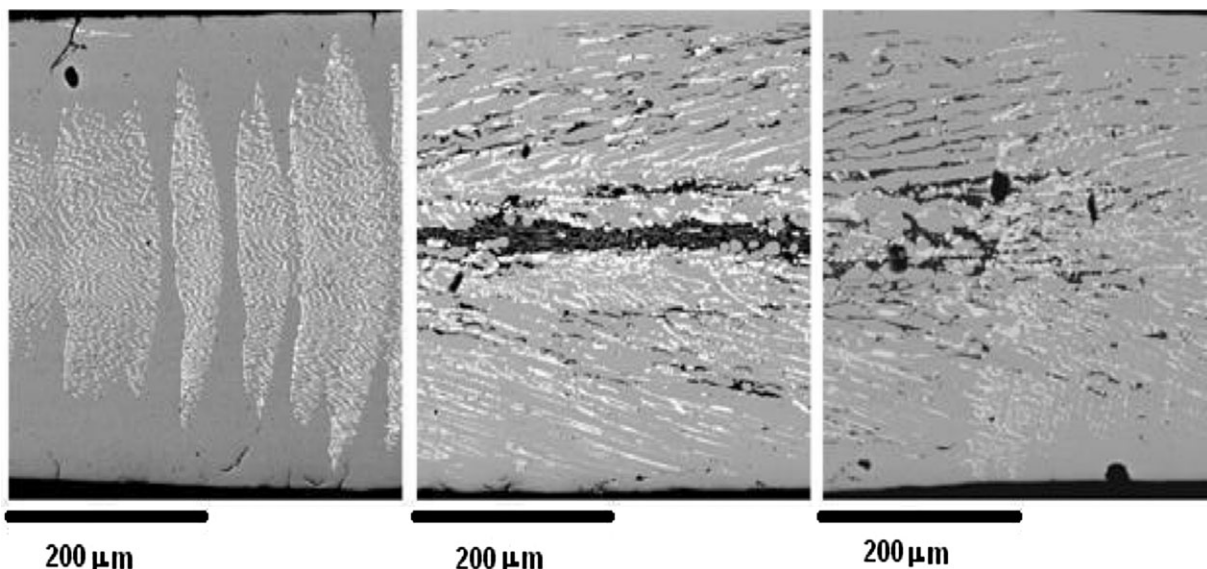


Figure 1 SEM images ($200\times$ magnification) of different regions of LCMO fiber, showing the evolution of the growth process (from the seed end at the left to the pedestal end at the right).

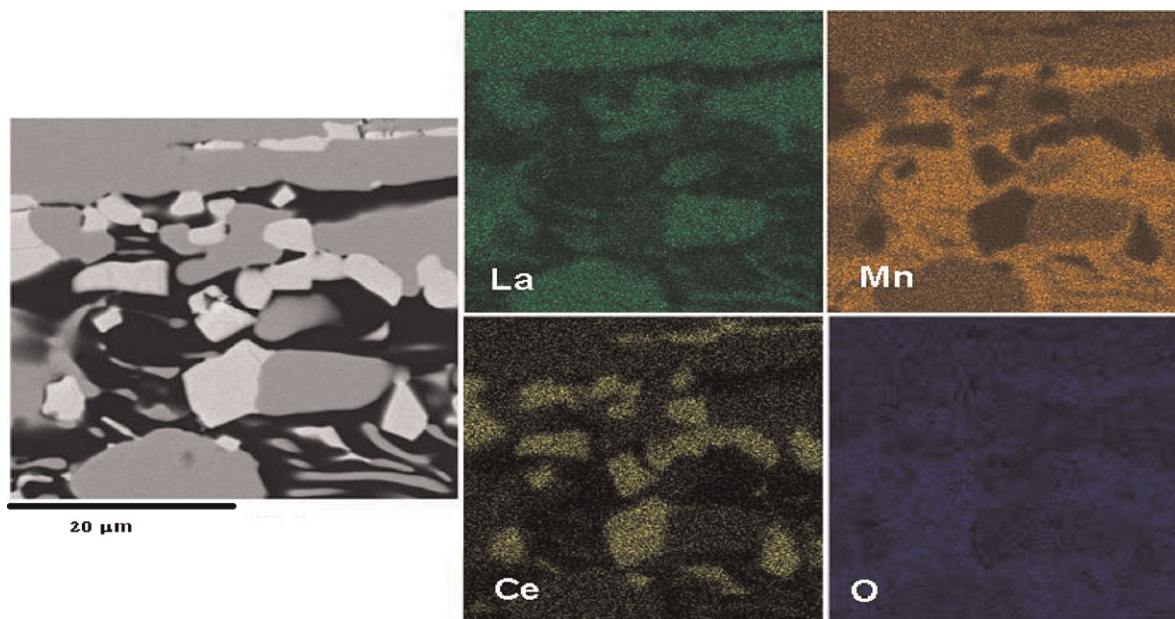


Figure 2 (online colour at: www.pss-a.com) SEM image ($2000\times$ magnification) and corresponding composition map of the LCMO fiber showing the presence of MnO_2 (black regions), CeO_2 (white regions), and the desired cerium doped manganite (gray regions).

magnetic contribution of other phases. It is interesting to point out that within this scenario we can treat a weak transition at $T_{C0} = 45$ K on the same footing as Ce mediated phase transitions by noting that with good accuracy [19] $T_{C0} \simeq 0.5T_C(x=0)$. Furthermore, to fit the experimental data, we subtract the contribution related to the broad transition at $T_{C,\text{max}} = T_C(x=0.3) = 300$ K by introducing the reduced magnetization $\Delta M(T, x) = M(T, x) - M_R(x =$

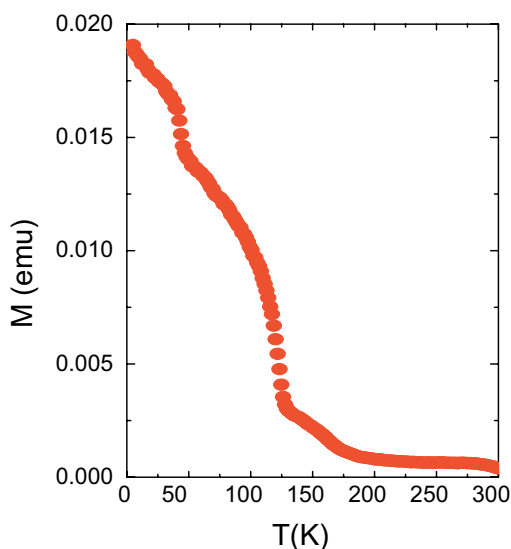


Figure 3 (online colour at: www.pss-a.com) Zero-field cooled M - T data for a piece of the central region of LCMO fiber. Four magnetic transitions can be identified with the Curie temperatures $T_{C0} = 45$ K, $T_{C1} = 126$ K, $T_{C2} = 180$ K, and $T_{C,\text{max}} = 300$ K.

$0.13)$. Figure 4 presents the best fits of the normalized reduced magnetization $\Delta M(T, x)/M(0, x)$ versus reduced temperature T/T_{C2} according to Eq. (1) with the following set of parameters: $T_{C0} = 0.5T_C(0) = 45$ K, $T_{C1} = T_C(0.063) = 126$ K, $T_{C2} = T_C(0.13) = 180$ K, $M_0(0) = 0.95M(0, 0)$, $M_0(0.063) = 0.5M(0, 0)$, $M_0(0.13) = 0.25M(0, 0)$, $M_R(0) = 0.05M(0, 0)$, $M_R(0.063) = 0.01M(0, 0)$, and $M_R(0.13) = 0.005M(0, 0)$ where $M(0, 0) = 0.019$ emu is the absolute

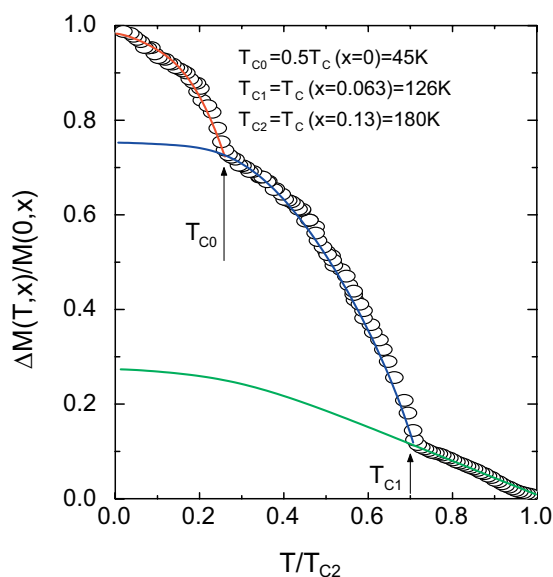


Figure 4 (online colour at: www.pss-a.com) The best fits of the normalized reduced magnetization $\Delta M(T, x)/M(0, x)$ versus reduced temperature T/T_{C2} according to Eq. (1), showing three transitions.

value of the measured magnetization at the lowest temperature (see Fig. 3). Finally, it is important to mention that within the spin polaron scenario, the same magnetization $M(T, x)$ is also responsible for anomalous resistivity of doped manganites [24] $\rho(T, x) \propto e^{-\gamma M^2(T, x)}$ with $\gamma \propto 1/M_0^2(x)$.

4 Conclusions In summary, a possibility to grow polycrystalline bulk-type LCMO manganite fibers by using the highly energetic LHPG technique was presented. The performed EDX measurements clearly identified the presence of cerium atoms in our fibers responsible for three ferromagnetic transitions at 126, 180, and 300 K.

Acknowledgements We thank Dr. O. F. de Lima for providing the facilities for the magnetic characterization of our samples and useful discussions. The authors gratefully acknowledge the financial support from Brazilian Agencies FAPESP, CAPES, and CNPq.

References

- [1] Y. Tokura (ed.), *Colossal Magnetoresistive Oxides* (Gordon and Breach, New York, 2000).
- [2] C. N. R. Rao and B. Raveau (eds.), *Colossal Magnetoresistance, Charge Ordering and Related Properties of Manganese Oxides* (World Scientific, Singapore, 1998).
- [3] J. P. Zhou, J. T. McDevitt, J. S. Zhou, H. Q. Yin, J. B. Goodenough, Y. Gim, and Q. X. Jia, *Appl. Phys. Lett.* **75**, 1146 (1999).
- [4] N. Moutis, I. Panagiotopoulos, M. Pissas, and D. Niarchos, *Phys. Rev. B* **59**, 1129 (1999).
- [5] M. Rubinstein, D. J. Gillespie, J. E. Snyder, and T. M. Tritt, *Phys. Rev. B* **56**, 5412 (1997).
- [6] H. Y. Hwang, S.-W. Cheong, P. G. Radaelli, M. Marezio, and B. Batlogg, *Phys. Rev. Lett.* **75**, 914 (1995).
- [7] J. C. Nie, J. H. Wang, and B. R. Zhao, *J. Magn. Magn. Mater.* **192**, L379 (1999).
- [8] P. Mandal and S. Das, *Phys. Rev. B* **56**, 15073 (1997).
- [9] J. Philip and T. R. N. Kutty, *J. Phys.: Condens. Matter* **11**, 8537 (1999).
- [10] P. Raychaudhuri, S. Mukherjee, A. K. Nigam, J. John, U. D. Vaisnav, R. Pinto, and P. Mandal, *J. Appl. Phys.* **86**, 5718 (1999).
- [11] J. R. Gebhardt, S. Roy, and N. Ali, *J. Appl. Phys.* **85**, 5390 (1999).
- [12] C. Mitra, P. Raychaudhuri, J. John, S. K. Dhar, A. K. Nigam, and R. Pinto, *J. Appl. Phys.* **89**, 524 (2001).
- [13] C. Mitra, P. Raychaudhuri, G. Kobernik, K. Dorr, K.-H. Muller, L. Schultz, and R. Pinto, *Appl. Phys. Lett.* **79**, 2408 (2001).
- [14] C. Mitra, P. Raychaudhuri, K. Dorr, K.-H. Muller, L. Schultz, P. M. Oppener, and S. Wirth, *Phys. Rev. Lett.* **90**, 017202 (2003).
- [15] C. Mitra, Z. Hu, P. Raychaudhuri, S. Wirth, S. I. Csiszar, H. H. Hsieh, H.-J. Lin, C. T. Chen, and L. H. Tjeng, *Phys. Rev. B* **67**, 092404 (2003).
- [16] R. Ganguly, I. K. Gopalakrishnan, and J. V. Yakhmi, *J. Phys.: Condens. Matter* **12**, L719 (2000).
- [17] C. Krishnamoorthy, K. Sethupathi, and V. Sankaranarayanan, *Mater. Lett.* **61**, 3254 (2007).
- [18] Z. Hu, R. Meier, C. Schüßler-Langeheine, E. Weschke, G. Kaindl, I. Felner, M. Merz, N. Nücker, S. Schuppler, and A. Erb, *Phys. Rev. B* **60**, 1460 (1999).
- [19] P. Raychaudhuri, C. Mitra, P. D. A. Mann, and S. Wirth, *J. Appl. Phys.* **93**, 8328 (2003).
- [20] S. W. Han, J.-S. Kang, K. H. Kim, J. D. Lee, J. H. Kim, S. C. Wi, C. Mitra, P. Raychaudhuri, S. Wirth, K. J. Kim, B. S. Kim, J. I. Jeong, S. K. Kwon, and B. I. Min, *Phys. Rev. B* **69**, 104406 (2004).
- [21] T. Yanagida, T. Kanki, B. Vilquin, H. Tanaka, and T. Kawai, *Phys. Rev. B* **70**, 184437 (2004).
- [22] C. A. Cardoso, F. M. Araujo-Moreira, M. R. B. Andreetta, A. C. Hernandez, E. R. Leite, O. F. de Lima, A. W. Mombrú, and R. Faccio, *Appl. Phys. Lett.* **83**, 3135 (2003).
- [23] M. R. B. Andreetta, L. C. Caraschi, and A. C. Hernandez, *Mater. Res.* **6**, 107 (2003).
- [24] S. Sergeenkov, H. Bougrine, M. Ausloos, and R. Cloots, *JETP Lett.* **69**, 858 (1999).
- [25] S. Sergeenkov, J. Mucha, M. Pekala, V. Drozd, and M. Ausloos, *J. Appl. Phys.* **102**, 083916 (2007).